

# A Noninvasive Integrative Method for Analyzing Radiation-Induced Lung Injury

Mariam P. Korah, MD  
 Anthony F. Waller  
 Eduard Schreiber, PhD  
 Walter J. Curran, Jr, MD  
 Ian R. Crocker, MD, FACR

*Department of Radiation Oncology, Emory University  
 School of Medicine, Atlanta, Georgia*

## Introduction

The efficacy of radiation treatment for intrathoracic malignancy is limited by the development of radiation-induced lung injury (RILI), which can cause radiation pneumonitis and fibrosis in the lung parenchyma. Several factors influence the risk and severity of RILI, including the radiation dose, the fractionation, the volume of irradiated lung, and whether the patient has pre-existing lung disease or has received systemic agents or prior thoracic radiation.<sup>1-3</sup>

Radiation pneumonitis usually manifests 1–6 months after completion of radiation, and it may progress to irreversible pulmonary fibrosis. Although radiographic changes sometime manifest with no accompanying symptoms, the classic triad includes dyspnea, cough, and fever, which respond to corticosteroid intervention.<sup>2,4</sup>

Radiologic findings are imprecise, yielding a broad differential diagnosis that may warrant pathologic verification and could delay initiation of management. Acute changes from radiation pneumonitis consist of a diffuse haze in the treatment region, ground-glass opacity, and consolidation. Late changes include traction bronchiectasis, volume loss, and scarring. A straight-line effect that conforms not to anatomic boundaries but rather to the margins of the radiation port is the most distinctive feature of RILI.<sup>4,5</sup> This case report describes a noninvasive integrative method used to carefully analyze radiation pneumonitis in the follow-up evaluation of a patient treated with chest radiotherapy.

## Case Report

A 46-year-old male smoker presented with cough and blood-tinged sputum. Positron emission tomography/computed tomography (PET/CT) imaging showed a 9 cm (anteroposterior) × 8 cm (transverse) mass replacing the right upper lobe of the lung, with a maximum standardized uptake value (SUV) of 16. Enlarged hypermetabolic mediastinal and contralateral hilar lymph nodes were present. The biopsy was diagnostic of non-small cell lung cancer. The patient was classified as T2, N3, M0, stage IIIB. Pretreatment pulmonary function testing (PFTs) showed that the forced expiratory lung volume in 1 second (FEV<sub>1</sub>) was 2.51 (58% of predicted), the forced vital capacity (FVC) was 3.38 (62% of predicted), and the diffusion capacity for carbon monoxide (DL<sub>CO</sub>) was 18.1 (45% of predicted).

After discussion among members of a multidisciplinary tumor board, definitive treatment with concurrent chemoradiation was initiated. Chemotherapy consisted of concurrent cisplatin 50 mg/m<sup>2</sup> intravenous (IV) on days 1, 8, 29, and 36 and etoposide 50 mg/m<sup>2</sup> IV on days 1–5 and 29–33. Radiation was delivered using megavoltage energy (6 MV) in daily fractionations of 1.8 Gy, for a total dose of 66.6 Gy. The gross tumor volume encompassed the gross tumor, lymph nodes exceeding 1 cm in short axis diameter on the CT scan, and all fluorodeoxyglucose-avid areas (with SUV >3) defined on PET. A modified 5 mm margin was added to generate a clinical target volume. An additional margin of 8 mm was given to create the initial planning target volume (iPTV). The boost PTV (bPTV) included the iPTV minus the mediastinum to spare dose to the spinal cord.

Radiation was delivered using 2 plans. Plan 1 delivered a dose of 36 Gy to the 96% isodose line (IDL) using anteroposterior-posteroanterior fields (AP-PA;

Address correspondence to:

Mariam P. Korah, MD, Department of Radiation Oncology, The Emory Clinic, 1365 Clifton Rd NE, Atlanta, GA 30322; Phone: 404-778-3473; Fax: 404-778-3670; E-mail: mariam.philip@gmail.com.

measuring  $22 \times 13$  cm in the x, y dimensions) to iPTV. Plan 2 delivered an additional 30.6 Gy, using AP-PA fields (measuring  $13 \times 12$  cm in the x, y dimensions) to the 97% IDL to bPTV. The treatment plan was generated using the Eclipse (Varian Medical Systems) treatment planning station (pencil beam algorithm, no heterogeneity corrections).

The patient tolerated treatment without breaks. PET/CT imaging 3 months after completion of chemoradiation showed a decrease in the size and SUV of the right upper lobe mass. PFTs showed the following values: FEV<sub>1</sub> of 2.60 (58% of predicted), FVC of 3.52 (62% of predicted), and DL<sub>CO</sub> of 17.1 (41% of predicted).

Four months following completion of radiation, the patient presented to the emergency room with dyspnea, cough, and low-grade fever. A CT scan showed new diffuse bilateral consolidation, ground-glass opacity, and increased septal lines in the right lung as compared with the left. The radiologist interpreted the findings as nonspecific, with the differential diagnosis including infection, lymphangitic or direct extension of tumor, pulmonary edema, and RILI.

Physicians in the radiation oncology unit were alerted to the change in the patient's pulmonary status and asked to determine whether radiation pneumonitis was a probable diagnosis. The on-call oncologist believed that the imaging changes were more likely to represent infection or disease progression. The patient underwent an extensive infectious disease work-up that included lung biopsy. While the results of these tests were awaited, we explored the possibility of radiation pneumonitis by determining the correspondence between the patient's dose wash and the radiographic changes. To that end, the CT simulation scan and dose matrix (in Digital Imaging and Communications in Medicine Radiology and Radiotherapy dose format) were exported from Eclipse. With the use of VelocityAI software (Velocity Medical Solutions), the simulation CT scan was registered to the relevant post-treatment diagnostic CT scan. After the physician manually aligned the images, they were fused using automated image registration. Image fusion was performed using a mutual-information rigid registration algorithm with 6 degrees of freedom and optimized using a physician-delineated region of interest. Once the anatomic imaging data from both CT volumes were fused, the registration was applied to the dose matrix, allowing the physician to view the previous dose region atop the new diagnostic image.

On visual inspection, it quickly became clear that the radiographic changes apparent on the new diagnostic CT scan approximated the boundaries of the 20 Gy IDL (Figure 1). The mean lung dose (MLD) and V<sub>20</sub> (the percentage of lung volume receiving a dose of

$\geq 20$  Gy) measured 20.6 Gy and 31.7%, respectively. A histogram of CT attenuation values, measured in Hounsfield units (HU), for lung volume within and outside the 20 Gy IDL was constructed with VelocityAI software. The median HU value was -275 (range: -678–297) in the lung volume receiving more than 20 Gy and -536 (range: -784–173) in the lung volume receiving less than 20 Gy (Figure 2).

Biopsy of the lung revealed a diffuse alveolar damage pattern of injury consistent with radiation pneumonitis, confirming the above analysis. The patient was subsequently initiated on steroid therapy, and respiratory symptoms promptly improved.

## Discussion

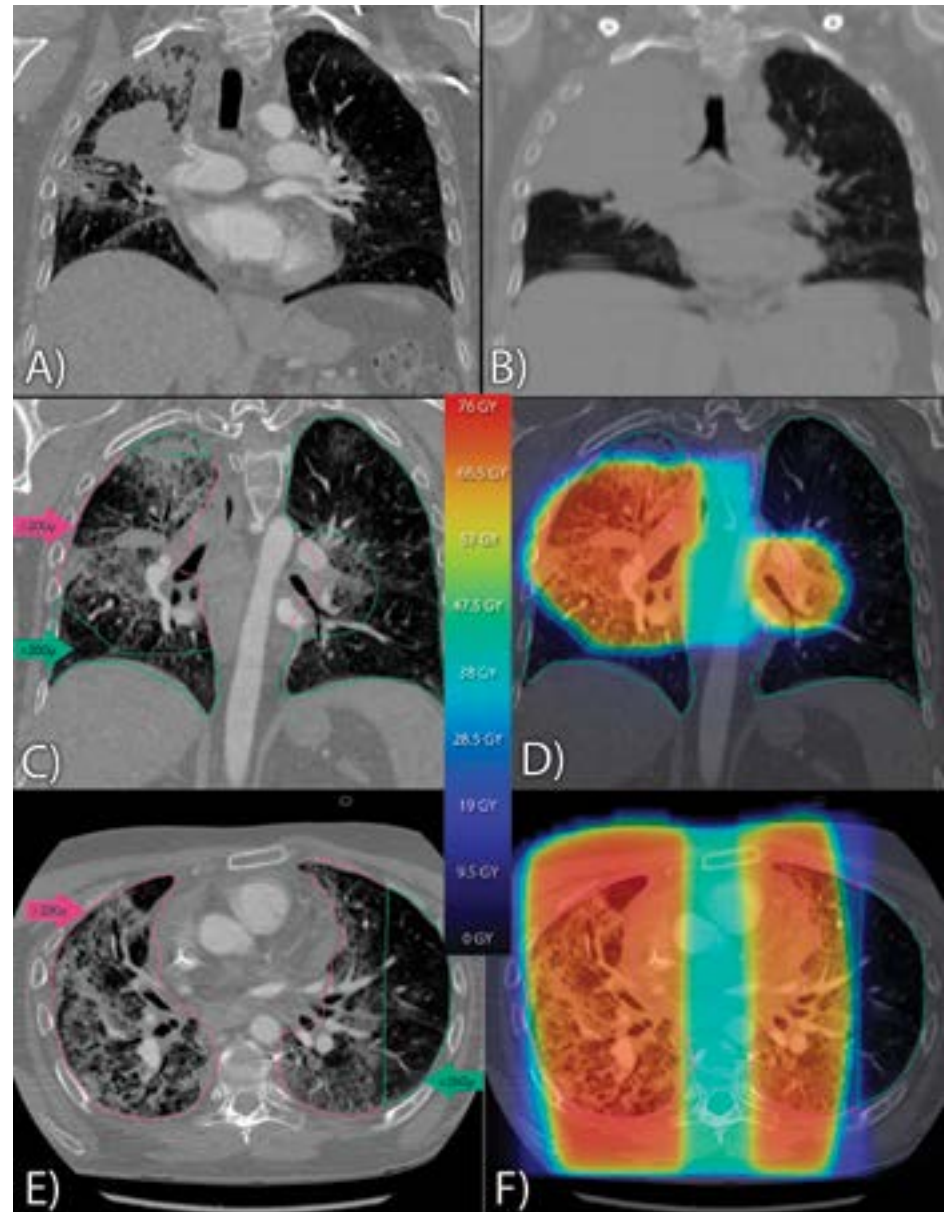
RILI is a dose-limiting toxicity in the management of malignant tumors of intrathoracic organs. Attempts to minimize complication risk have focused on treatment-specific factors. Normal tissue constraints are routinely applied to radiation treatment planning, and uninvolved lung parenchyma is an important area at risk during chest radiotherapy. Dose, volume, and fractionation are closely correlated to RILI. The MLD or V<sub>20</sub> are standard dosimetric indices for predicting lung toxicity. MLD exceeding 20 Gy and V<sub>20</sub> exceeding 37% are thought to be associated with unacceptable rates of RILI. Validation of dosimetric parameters is warranted in the combined modality setting, as certain systemic agents lower the threshold for induction of RILI.<sup>2-3,6</sup>

Failure to recognize the clinical and radiographic features of RILI can result in significant morbidity and possible mortality. Infection, comorbid pulmonary or cardiac disease, and tumor progression, which are conditions common to the treated population, present in a similar manner and can obscure an accurate diagnosis.<sup>2</sup>

A noninvasive approach for increasing the index of suspicion relies upon the pattern of radiation injury, which predictably mirrors the configuration of the radiation portal in most instances.<sup>4,5</sup> In addition, the CT attenuation histogram may be used as a quantitative measure of lung fibrosis. The relative amounts of air, soft tissue, and blood in each voxel determine CT attenuation. Lung attenuation will increase as a result of lung fibrosis and inflammation, which cause an increase in soft tissue in the lung. An increase in lung attenuation parallels worsening severity of radiation fibrosis.<sup>7-9</sup>

Visualization of a single image set in isolation and of pretreatment and post-treatment image sets in side-by-side comparisons is frequently suboptimal in the analysis of differences between scans. Spatially coregistered anatomic images offer a more refined approach. Moreover, an overlay of the dose matrix and a clearer understanding

**Figure 1.** Coronal registration images from the diagnostic computed tomography scan (A) and the pretreatment computed tomography simulation scan (B). Panels C–F show coronal and axial registration images of the superimposed dose matrix. The pink arrow delineates the region of lung receiving >20 Gy. The green arrow delineates the region of lung receiving <20 Gy.



of the physiologic lung function in affected areas afford better localization of the regions at greater risk for RILI. With early recognition, the complications can be effectively managed with simple medical interventions.

Our patient was initially admitted to the hospital because of increased oxygen requirements. Based on juxtaposed visualization of the prior treatment fields and scans, the consulting oncologist found that the new pattern of CT changes was not thought to be compatible with radiation pneumonitis. Disease progression or infection were the favored differential diagnoses. The patient received a course of broad-spectrum antibiotics, which

failed, and he then underwent a biopsy. After careful evaluation employing the composite method described above, radiation pneumonitis emerged as the top differential diagnosis. If this diagnosis had been reached sooner, steroid therapy could have been initiated earlier, providing immediate relief of symptoms and thereby avoiding unnecessary interventions.

### Conclusion

An integrative software tool that links geometric, functional, and dosimetric information among serial scans

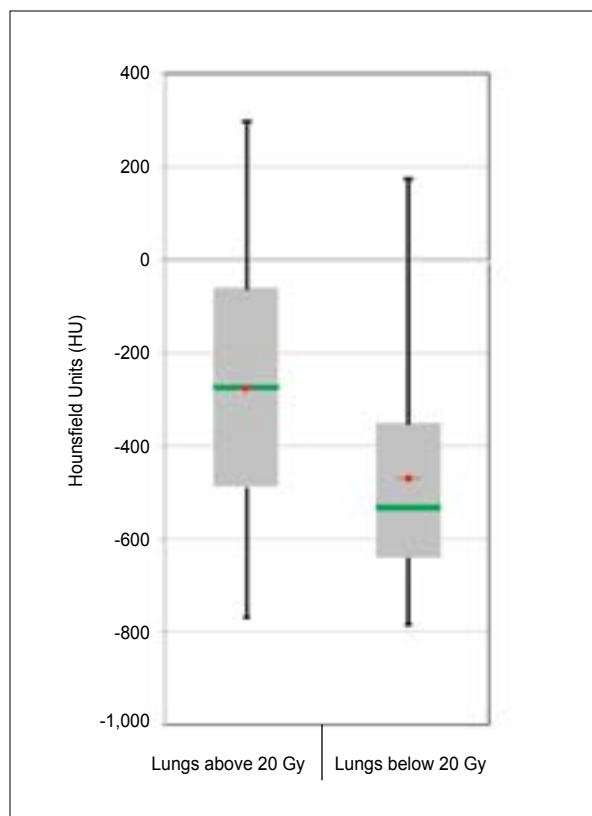


**Figure 2.** Box and whisker plot of computed tomography attenuation values (measured in Hounsfield units) of the radiation treatment volume receiving doses of greater than or less than 20 Gy. The red diamond depicts the mean values. The green line depicts the median values.

permits more thorough inspection and is superior to a side-by-side comparison of the same data. As illustrated in this case report, the application of such a system ultimately streamlines the physician's ability to arrive at an accurate clinical diagnosis. Robust noninvasive methods such as this one may spare patients the risks associated with biopsy and allow early and effective treatment intervention.

#### Acknowledgment

*Dr. Crocker is entitled to receive royalty payments on sales of VelocityAI software (Velocity Medical Solutions) through an intellectual property agreement between Velocity Medical Solutions and Emory University.*

#### References

1. Groover TA, Christie AC, Merritt EA. Observations on the use of the copper filter in the treatment of deep-seated malignancies. *South Med J.* 1922;15:440-444.
2. Movsas B, Raffin TA, Epstein AH, et al. Pulmonary radiation injury. *Chest.* 1997;111:1061-1076.

3. Roach M III, Gandara DR, Yuo HS, et al. Radiation pneumonitis following combined modality therapy for lung cancer: analysis of prognostic factors. *J Clin Oncol.* 1995;13:2606-2612.
4. Rosiello RA, Merrill WW. Radiation-induced lung injury. *Clin Chest Med.* 1990;11:65-71.
5. Choi YW, Munden RF, Erasmus JJ, et al. Effects of radiation therapy on the lung: radiologic appearances and differential diagnosis. *Radiographics.* 2004;24:985-997.
6. Bradley J. A review of radiation dose escalation trials for non-small cell lung cancer within the Radiation Therapy Oncology Group. *Semin Oncol.* 2005;32:111-113.
7. Rosen II, Fischer TA, Antolak JA, et al. Correlation between lung fibrosis and radiation therapy dose after concurrent radiation therapy and chemotherapy for limited small cell lung cancer. *Radiology.* 2001;221:614-622.
8. Guerrero T, Castillo R, Noyola-Martinez J, et al. Reduction of pulmonary compliance found with high-resolution computed tomography in irradiated mice. *Int J Radiat Oncol Biol Phys.* 2007;67:879-887.
9. Lynch DA. Quantitative CT of fibrotic interstitial lung disease. *Chest.* 2007;131:643-644.

## Review

### Assessment of Radiation-Induced Lung Disease

Jacqueline P. Williams, PhD

*University of Rochester Medical Center,  
Rochester, New York*

#### Introduction

Radiation pneumonitis and pulmonary fibrosis are the potentially lethal acute and late effects, respectively, that are the frequent and unfortunate outcomes following radiation therapy involving the thoracic volume. Indeed, the incidence of radiation pneumonitis in lung cancer patients receiving radiotherapy ranges from 5–50%,<sup>1</sup> which has led to considerable limitations in the ability of radiation oncologists to deliver a maximally effective dose for tumor treatment, reducing the probability of eradication. Therefore, this dose-limiting sensitivity of the lung has led to significant efforts, at both the preclinical and clinical levels, to identify the factors that contribute to or further exacerbate the initiation and progression of injury and the development of radiation-induced lung disease (RILD) in pulmonary normal tissues.

Address correspondence to:

Jacqueline P. Williams, PhD, University of Rochester Medical Center, 601 Elmwood Avenue, Box 647, Rochester, NY 14642; E-mail: Jackie\_Williams@URMC.Rochester.edu.

## Assessment of Radiation-Induced Lung Disease

A significant number of factors are thought to contribute to the development of RILD. Technique-related factors include the volume of lung irradiated, the total mean dose delivered, and the fractionation schedule; patient factors include the use of chemotherapeutic agents, age, sex, and smoking status. At the clinical level, the dose-volume relationship has been of considerable interest as a predictive parameter for RILD development. For example, various investigators have identified threshold levels associated with the  $V_{20}$  (volume receiving  $\geq 20$  Gy),<sup>2</sup>  $V_{30}$ ,<sup>3</sup> and/or  $V_{40}$ ,<sup>4</sup> as well as the mean lung dose,<sup>5</sup> providing critical treatment constraints that can be used to predict the probability of the development of pulmonary late effects, in particular, pneumonitis. However, an alternative use of these dosimetric parameters, as described by Korah and colleagues,<sup>6</sup> is to confirm the presence of RILD for treatment purposes.

Since a classically recognized characteristic of radiation pneumonitis is its conformation to the treatment portal, this feature is often used to assist with diagnosis. However, although radiologic manifestations of RILD are well described—involving ground-glass opacities and consolidations in the acute and late phases—firm diagnosis is frequently a difficult task given the plethora of differential conditions that may provide confounding factors, including anemia, cardiac arrhythmia, infection, and radio-induced or recurrent tumor.<sup>7</sup> Nonetheless, as recently described in an elegant paper from Jeraj and associates,<sup>8</sup> imaging offers the potential of a noninvasive means of monitoring normal tissue damage, providing qualitative assessments at the anatomic (structural) level. However, as Korah and colleagues rightly note, when such techniques are used in the lung, the comparison between pretreatment and post-treatment images is frequently suboptimal due to a number of factors, including image deformation from respiration and anatomic changes due to normal tissue remodeling or tumor shrinkage.<sup>5</sup> Thus, Korah and colleagues described a coregistration approach using anatomic images that, together with manual alignments made by the physician, gave optimal image fusion.<sup>6</sup> This technique provided the team with the ability to more accurately arrive at a diagnosis of RILD because it gave confirmation of radiographic changes occurring within the 20 Gy isodose line. The patient was successfully treated with steroids and demonstrated improved respiration.

Such methodologies, however, do not allow for early intervention and quicker amelioration of RILD. In attempts to develop such strategies, other investigators have looked at lung function as a surrogate marker of ongoing disease, with some studies showing a weak

correlation between regional lung perfusion/density (as measured by single-photon emission computed tomography).<sup>9</sup> A recent study indicated that some of the same confounding factors that reduce the efficacy of anatomic-based imaging may also affect functional assessments.<sup>10</sup> Alternative imaging techniques that allow monitoring of functional and molecular parameters, such as fluorodeoxyglucose positron emission tomography and functional magnetic resonance imaging, may ultimately provide more clinically important findings because they more accurately reflect the ongoing clinical processes.<sup>8</sup> Such techniques require an intimate knowledge of the physiologic and pathologic processes underlying RILD; in order for them to act as surrogates of the disease, the clinician must be able to correlate imaging markers with clinical endpoints.

## Ameliorating Radiation-Induced Lung Disease

Radiation pneumonitis and pulmonary fibrosis are not singular pathologic entities. They are the endpoints of progressive changes within the lung parenchyma and represent pathways that result in chronic inflammation and/or tissue remodeling. Although both entities are associated with dysregulated wound healing and immune response, the relationship between the 2 endpoints is yet to be firmly established. Nonetheless, with respect to the abrogation of RILD, the most prudent course of action to prevent onset and expression is to provide radioprotection to the normal tissues—although there has been little to no success in this area to date.<sup>5</sup> An alternative approach would be to mitigate the progression of the injury, an area of research that is currently under considerable investigation.

Not surprisingly, preclinical studies have shown that there is increased cytokine and growth factor expression within hours of radiation delivery, with accompanying localized increases in inflammatory cell infiltration.<sup>11</sup> Although it is not unreasonable to presume that these events are part of the immediate tissue response to radiation-induced cell death and are, therefore, part of canonical wound healing pathways,<sup>12</sup> it has been argued that normal tissue late-effect initiation, progression, and development are part of a continuum.<sup>13</sup> Cyclical upregulation of cytokine and growth factor expression, seen both in the localized injured tissue and systemically in the circulation during the so-called latent period prior to RILD, has been demonstrated at both the bench and clinical levels.<sup>14</sup> Their ultimate association with pathologic events, including increased inflammation and the onset of fibrosis, suggests that such signals not only may be used as surrogate markers of disease, but also may act as targets for mitigation of RILD. Such findings offer encouragement

that strategies can be developed that will identify normal tissue injury progression prior to the onset of symptoms, forestalling the need for subsequent differential diagnosis evaluation.

## Conclusion

Integrated methodologies that make use of anatomically-based imaging currently offer additional assistance to oncologists to confirm the onset of RILD in order to provide timely administration of symptomatic treatment. However, earlier intervention would reduce patient stress and prevent unwanted side effects from agents such as steroids. Increased focus should, therefore, be applied to the identification of correlative biomarkers that would provide an early signal of the increased probability of late effect development. Success in this area would improve patient quality of life by providing the ability to intervene prior to symptom onset, thereby minimizing the risk of misdiagnosis and, possibly, identifying more targeted mitigating strategies.<sup>15</sup>

## References

1. Marks LB, Yu X, Vujaskovic Z, et al. Radiation-induced lung injury. *Semin Radiother Oncol.* 2003;13:333-345.
2. Ramella S, Trodella L, Mineo TC, et al. Adding ipsilateral V20 and V30 to conventional constraints predicts radiation pneumonitis in stage IIIA-B NSCLC treated with combined-modality therapy. *Int J Radiat Oncol Biol Phys.* 2010;76:110-115.
3. Hernando ML, Marks LB, Bentel GC, et al. Radiation-induced pulmonary toxicity: a dose-volume histogram analysis in 201 patients with lung cancer. *Int J Radiat Oncol Biol Phys.* 2001;51:650-659.
4. Willner J, Jost A, Baier K, et al. A little to a lot or a lot to a little? An analysis of pneumonitis risk from dose-volume histogram parameters of the lung in patients with lung cancer treated with 3-D conformal radiotherapy. *Strahlenther Onkol.* 2003;179:548-556.
5. Marks LB, Bentzen SM, Deasy JO, et al. Radiation dose-volume effects in the lung. *Int J Radiat Oncology Biol Phys.* 2010;76(3 suppl):S70-S76.
6. Korah MP, Waller AF, Schreiber E, Curran Jr WJ, Crocker IR. A noninvasive integrative method for analyzing radiation-induced lung injury. *Clin Adv Hematol Oncol.* 2011;9:157-160.
7. Mehta V. Radiation pneumonitis and pulmonary fibrosis in non-small-cell lung cancer: pulmonary function, prediction, and prevention. *Int J Radiat Oncol Biol Phys.* 2005;63:5-24.
8. Jeraj R, Cao Y, Ten Haken RK, Hahn C, Marks L. Imaging for assessment of radiation-induced normal tissue effects. *Int J Radiat Oncology Biol Phys.* 2010;76(3 suppl):S140-S144.
9. Mao J, Zhang J, Zhou S, et al. Relating changes in pulmonary function tests (PFTs) to changes in radiation-induced regional lung perfusion. *Med Phys.* 2006;33:2151-2152.
10. Zhang J, Ma J, Zhou S, et al. Radiation-induced reductions in regional lung perfusion: 0.1-12 year data from a prospective clinical study. *Int J Radiat Oncol Biol Phys.* 2010;76:425-432.
11. Johnston CJ, Hernady E, Reed C, et al. Early alterations in cytokine expression in adult compared to developing lung in mice after radiation exposure. *Radiat Res.* 2010;173:522-535.
12. McBride WH, Chiang C-S, Olson JL, et al. A sense of danger from radiation. *Radiat Res.* 2004;162:1-19.
13. Rubin P, Johnston CJ, Williams JP, et al. A perpetual cascade of cytokine postirradiation leads to pulmonary fibrosis. *Int J Radiat Oncol Biol Phys.* 1995;33:99-109.
14. Chen Y, Hyrien O, Williams J, et al. Interleukin (IL)-1A and IL-6: applications to the predictive diagnostic testing of radiation pneumonitis. *Int J Radiat Oncol Biol Phys.* 2005;62:260-266.
15. Bentzen SM, Parliament M, Deasy JO, et al. Biomarkers and surrogate endpoints for normal-tissue effects of radiation therapy: the importance of dose-volume effects. *Int J Radiat Oncol Biol Phys.* 2010;76(3 suppl):S145-S150.